

# EXPERIMENTAL INVESTIGATION AND NUMERICAL SIMULATION OF THE FLOW AROUND AN AUTOMOTIVE MODEL: AHMED BODY

**Ivan Korkischko**

ivan.korkischko@poli.usp.br

**Julio Romano Meneghini**

jmeneg@usp.br

Departamento de Engenharia Mecânica - Escola Politécnica da Universidade de São Paulo - Av. Prof. Mello de Moraes, 2231 - São Paulo - SP - 05508-900, Brasil

**Abstract.** *In the last decades, the detailed knowledge of the flow characteristics around ground vehicles, such as cars, trucks, trains, motorcycles and bicycles, is considered of great importance to the adequate project of those vehicles, allowing improvements of energetic efficiency and dynamic characteristics. To achieve these objectives, experimental results and numerical simulations are of great importance. The present investigation covers experimental and the numerical parts of an aerodynamic project of a ground vehicle, using a simplified automotive model, the Ahmed body, which has great coverage in the literature. The experimental part involved drag measurement and flow visualization using PIV/LASER (Particle Image Velocimetry). Blockage effects were investigated and estimated on the basis of drag measurements. Flow visualization around the model was concentrated in the rear end of the model and the wake structure, which is the major responsible of the model's drag. The computational part consists of numerical simulations of the flow around the Ahmed body employing CFD (Computational Fluid Dynamics) techniques. The Finite Volume Method was used. Different turbulence models used in CFD problems were validated during these activities. Experimental results of drag measurements corrected of blockage effects have great agreement with results found in Ahmed and other references ( $C_D = 0.38$ ). The wake structures visualized with PIV also presented good agreement with other experimental studies. In numerical simulation results, three turbulence models were tested,  $k - \omega$  Standard,  $k - \omega$  SST and Spalart-Allmaras. The last two models have had excellent agreement with Ahmed's results in steady flow simulations. The  $k - \omega$  Standard model has shown poor results. Only the  $k - \omega$  SST model has had excellent agreement in unsteady flow simulations.*

**Keywords:** *Ahmed body, Experimental Fluid Mechanics, Particle Image Velocimetry, Computational Fluid Dynamics, Finite Volume Method*

## 1. INTRODUCTION

Even though the flow around bluff bodies is an elementary fluid mechanics problem, it presents great challenges due to its wide engineering applications. Bluff bodies are bodies where the flow is dominated by great separated flow regions. Different structures in most engineering fields are presented as bluff bodies immersed in fluid flows, like chimney stacks, tubes in heat exchangers, bridge piers, offshore platforms, skyscrapers, cars, airplanes, ships, among many others.

Many fundamental studies are presented trying to understand the dynamic interaction between body and flow, including this paper, which studies an automotive model. The Ahmed body (Ahmed, 1984) is extremely important to the automotive industry because it serves as wind tunnel calibration and CFD turbulence model benchmark.

Experimental research is fundamental to understand the existing phenomena in the flow around bluff and slender bodies and also as a method of validation of theoretical and numerical studies in fluid-dynamic problems. However, industries are using increasingly more computational methods aiming diminish the necessity of experiments. Because of high financial and temporal costs of experiments, the tendency of different industries is to invest massively in computational solutions, testing countless configurations, and just use experiments for final decisions of projects, or tests of the chosen solution, or to validate numerical models. In certain cases, the computational simulations can be impracticables or too time-consuming, then experiments can be more adequate to obtain results.

Trying to reproduce the methodology used in most important industries, like aerospace, automotive, offshore, an others, this paper utilize experimental and numerical methods. It is well known that one method does not substitute the other, but they are complementary and generate better projects. Considering what was already presented, this paper has the following objectives:

- Understand the drag mechanism in bluff bodies and obtain experimentally Ahmed body's drag coefficient.
- Obtain the wake structure of the chosen Ahmed body configuration with DPIV/Laser.
- Use experimental results to validate numerical simulations.
- Verify differences between the most employed turbulence models to external flows.

## 2. AHMED BODY

The geometry of a simplified automotive model proposed by Ahmed (1984), known as Ahmed body (Fig. 1), generates the essential features of a real vehicle flow field, with the exception of the effects due to the rotating wheels, engine and passenger compartment flow, rough underside, and surface projections, like mirrors. The chosen model generates: an strong three-dimensional flow in front, a relatively uniform flow in the middle, and a large structured wake at the rear (Ahmed, 1984).

The choice of an Ahmed body model also allows validation of turbulence numerical models. The variation of the rear slant angle  $\varphi$  of the Ahmed body (Fig. (1)) allows the obtention of various wake structures at the rear, which are responsible for the majority of the drag of the model, and also for surface vehicles, like cars, buses and trucks.

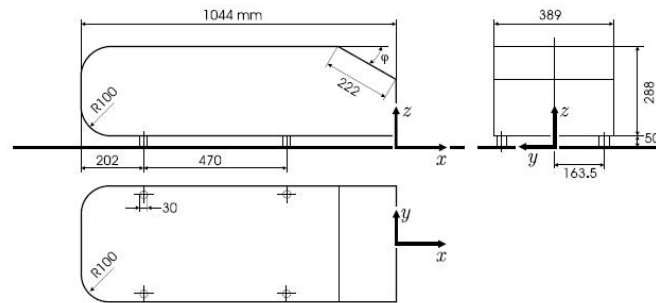


Figure 1. Ahmed body. Dimensions in mm. Reproduced from Hinterberger (2004)

## 3. EXPERIMENTAL ARRANGEMENT

The model used in experiments has a rear slant angle  $\varphi = 30^\circ$ , which presents maximum drag (Fig. 2). The model dimensions represent a 36 % scale from the original Ahmed body. The width of the model equals 1/5 of the width of NDF's circulating water channel. The model was made of a block of low-density polyurethane (Fig. 3(a)) coated with automotive plastic mass and automotive black painting. The finished model is presented in the Fig. 3(b).

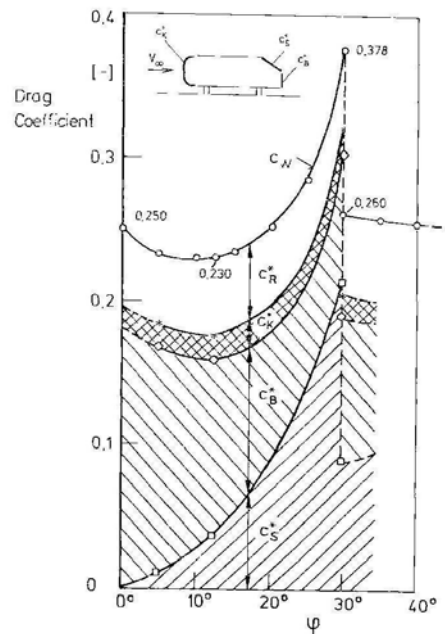
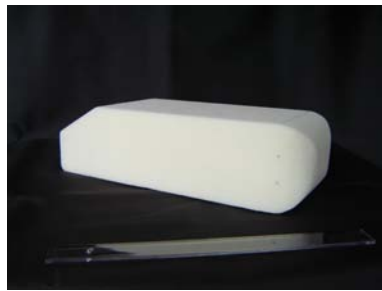


Figure 2. Variation of drag with rear slant angle  $\varphi$ . Reproduced from Ahmed (1984)

The Ahmed model is mounted in a structure above a circulating water channel (Fig. 4(a)) which has a test-section 0.7 m wide, 0.9 m deep and 7.5 m long. The flow velocity could be increased up to 1.0 m/s. The channel presents mean turbulence intensity  $TI = 0.022 \pm 0.004$ . The model is positioned in the first third of the test section length as in Fig. 4.



(a) Low-density polyurethane Model  $r = 36\%$

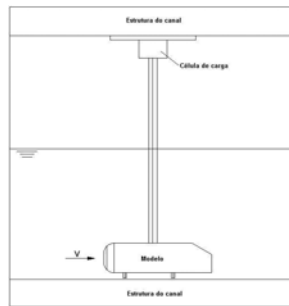


(b) Finished  $r = 36\%$  model

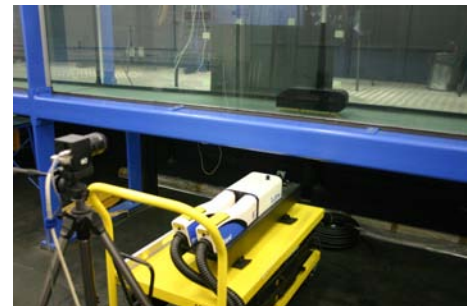
Figure 3. Ahmed body model



(a) Circulating water channel



(b) Schematic drawing



(c) Model and part of instrumentation

Figure 4. Experimental setup in circulating water channel

Drag measurements are made by a uniaxial load cell (ALFA Instrumentos S-5) mounted between the model and the supporting structure (Fig. 4(b)). Flow velocity is measured by a electromagnetic flowmeter (SIEMENS SITRANS F M MAGFLO MAG5000/MAG3100 W). Data acquisition and signal processing are handled by a National Instruments system (NI SCXI 1000, 1531, 1302 and 1314 modules and LabVIEW 7.1 software) and a Matlab code. Reynolds number for drag measurements is between  $4.2 \times 10^4$  and  $2.2 \times 10^5$ . Each data acquisition series has 200 s with a data acquisition frequency of 100 Hz.

The PIV-Laser (Particle Image Velocimetry) system was composed by a light source (laser), a camera, a dedicated computational system and particles that are in the flow. The flow is illuminated in a interest zone by a laser pulse plane. The image is captured by a camera that had a charged-coupled device (CCD) matrix, and was orthogonally positioned to the illuminated plane. The images were transmitted to a computer, where they are processed to obtain a vectorial field. The Laser is Quantel Brilliant Twins, synchronizer (LaserPulse), camera (PowerView 4 Megapixels) and software (Insight v. 3.53) are from TSI. Tracking particles are 12-11  $\mu\text{m}$  polyamide (Degussa). Images are captured at 4Hz, the interval between laser pulses is  $\Delta t = 1000 \mu\text{s}$ , and the interrogation window is  $64 \times 64$  pixels. PIV images are taken in the rear wake region.

Blockage effects result in the increase of the flow velocity around the body and in the wake. Blockage affects drag, lift and side forces, and it is important for all bodies with a blockage ratio,  $S/A$ , greater than 1%, where  $S$  is the model cross-sectional area, and  $A$  is the tests cross-sectional area. The Ahmed model used in this paper has a blockage ratio,  $S/A = 6.9\%$ , and, according to ESDU (2005), the most appropriated correction method for blockage effects in drag coefficient ( $C_D$ ) is the Quasi-streamlined Flow Method.

## 4. EXPERIMENTAL RESULTS

### 4.1 Drag measurements

Reynolds number for drag measurements is between  $4.2 \times 10^4$  and  $2.2 \times 10^5$ . The values of drag coefficient,  $C_D$ , and blockage-effect corrected drag coefficient,  $C_{Df}$ , are corrected considering the drag generated by the model support. Drag coefficient values obtained for  $\varphi = 30^\circ$  are:  $C_D = 0.515$  and  $C_{Df} = 0.383$ . Drag coefficient was  $C_D = 0.378$ , that is the biggest drag case, for the experimental study carried by Ahmed (1984), as shown in Fig. 2, and from the total drag, 85% is pressure drag, and 15%, friction drag. Comparing results from the present investigation with results from Ahmed (1984),  $C_D$  is 36% greater, and  $C_{Df}$ , which is corrected from blockage effects and model support drag, is 1% greater. This clearly indicates the validity of these corrections.

## 4.2 Flow visualization around the Ahmed body

The Particle Image Velocimetry (PIV-Laser) technique is used for flow visualization around the Ahmed body. Reynolds number is  $9.8 \times 10^4$  with uniform flow velocity and the body length as reference.

Knowing that the majority of the drag of a bluff body is generated by separation in the rear region of the body and formation of the vortices wake structure, the flow visualization study is focused in this region. The velocity field is measured in five horizontal planes and five vertical planes, all longitudinal to the flow direction, as shown in Fig. 5. PIV 2D velocity vectors are converted in flow vorticity and streamtraces. Figures 6 and 7 summarize PIV results, and show some wake structures of the rear of the Ahmed body. Despite the wake flow of a bluff body is basically unsteady, the time averaged flow exhibits macrostructures that appear to govern the pressure drag created at the rear end (Ahmed, 1984). The main characteristics of this flow can be seen in Fig. 8. Figure 6 shows a main structure: the shear layer, which comes off the rear slant side, rolls up in a longitudinal vortex, identified as vortex C in Fig. 8, in a similar way to the phenomenon observed on the wing tip of low aspect wings. In Fig. 7, at the top and bottom edges of the flat vertical base, the shear layer rolls up into two recirculatory flow regions A and B, situated one over another. The A and B vortices regions can also be verified in Fig. 6. These structures can be seen for different rear slant angles in Lienhart, Stoots and Becker (2000) and Okada, Sheridan and Thompson (2005).

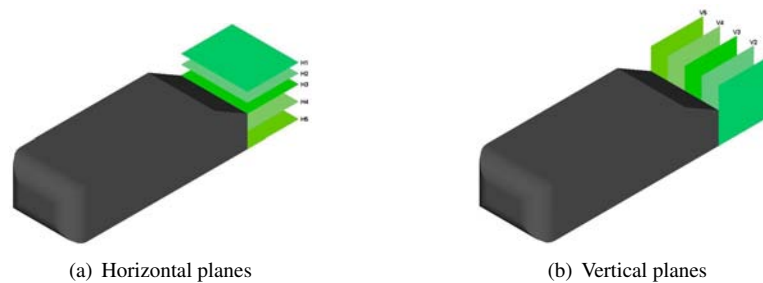


Figure 5. PIV measurement planes

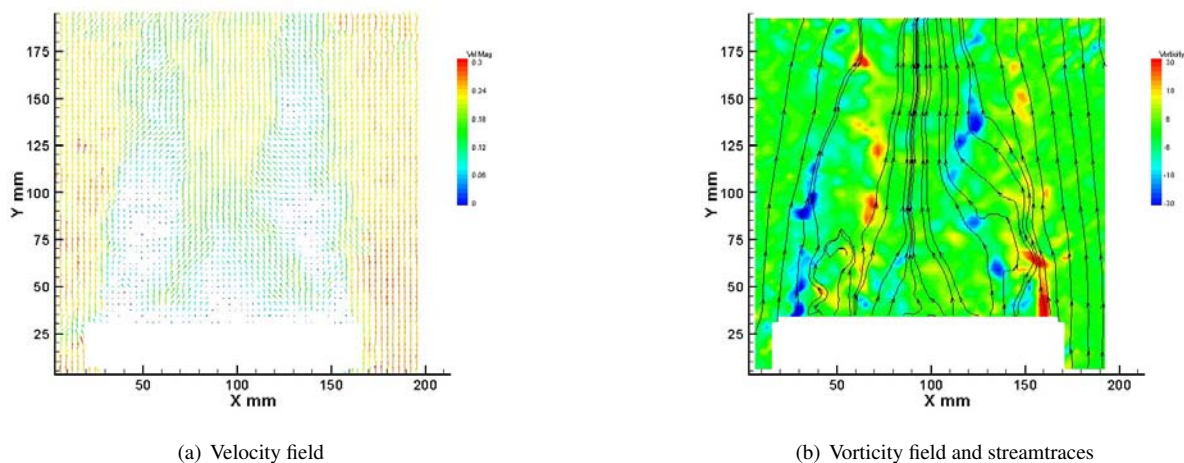


Figure 6. Flow around the Ahmed body in the horizontal plane (H5)

## 5. NUMERICAL SIMULATIONS

The Computational Fluid Dynamics (CFD) technique based in Finite Volume Method (FVM) is used in numerical simulations. The mesh is generated in the GAMBIT 2.1.2 software and numerical simulations are made in the FLU-ENT 6.2.16 software. Further information about these softwares can be found in Fluent (2000) and Fluent (2005). The numerical solution of the flow around the Ahmed body is obtained by steady and unsteady numerical simulations.

It can be found in literature papers presenting different methods of numerical simulation other than RANS, which is used in this paper. In Kapadia, Roy and Wurtzler (2003) and Krajnovic and Davidson (2004) there are numerical simulation results using DES, LES and different rear slant angles.

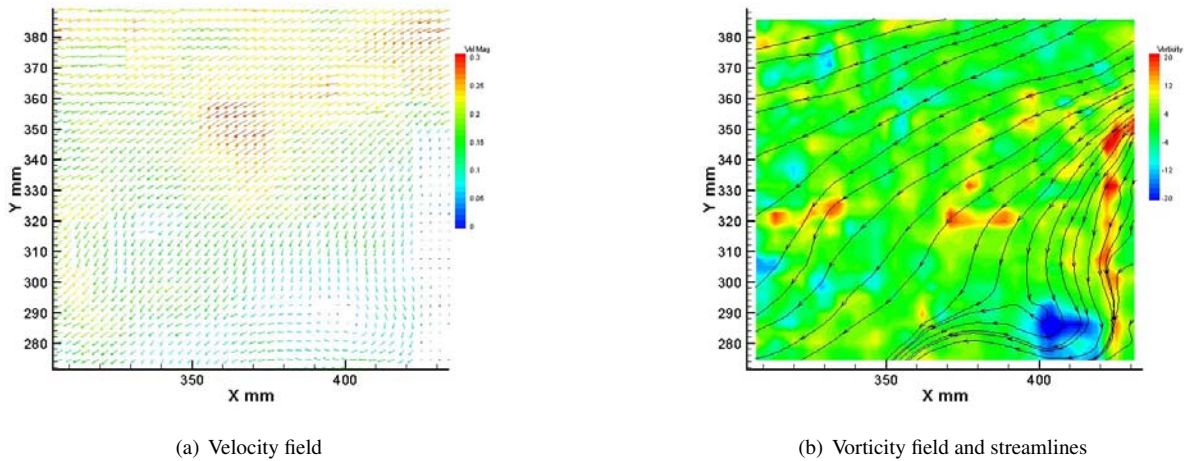


Figure 7. Flow around the Ahmed body in the vertical plane (V5)

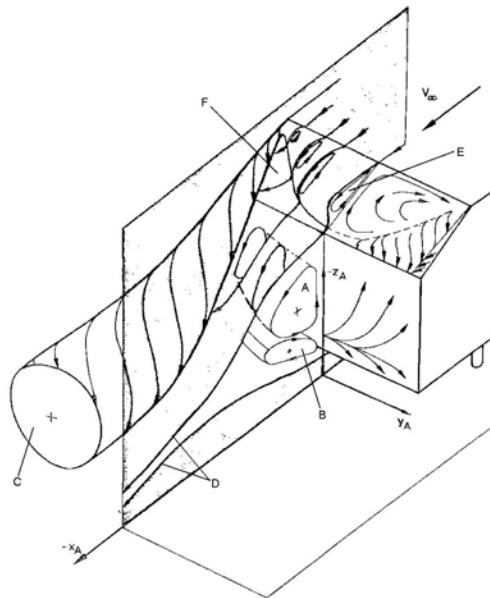


Figure 8. Schematic representation of high drag flow ( $\varphi = 30^\circ$ ). Reproduced from Ahmed (1984)

### 5.1 Mesh generation

The mesh generated in GAMBIT represents a domain of  $12L \times 4L \times 3L$  (length  $\times$  width  $\times$  height), based in the length  $L$  of model. The model is 50 mm above the floor. The unstructured mesh is composed of 1562877 tetrahedral elements. Figures 9 and 10 show the generated mesh. Boundary conditions are the following: uniform velocity at inlet, uniform pressure at outlet, symmetry at lateral and at top, wall at the model and moving wall at floor.

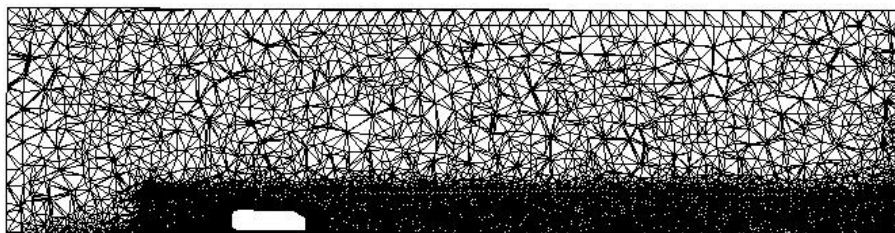


Figure 9. Longitudinal cut in the Ahmed body mesh



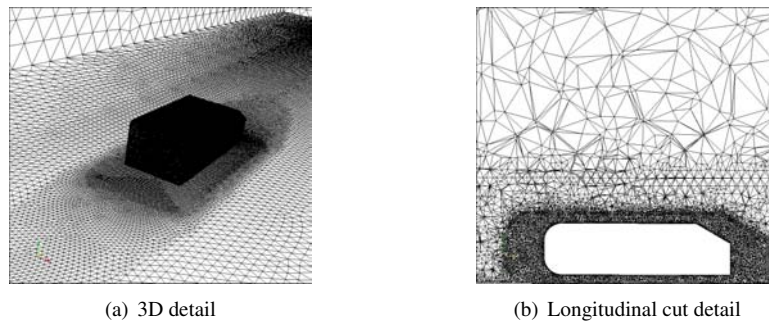


Figure 10. Ahmed body mesh details

## 5.2 Steady flow numerical simulations

Computational resources for the steady flow numerical simulations are a Compaq Alpha Server DS20E workstation (2 CPUs Alpha EV67 667 MHz and 4GB RAM) and Tru64 Unix V5.1 OS.

Inlet velocity  $V = 30\text{m/s}$  and zero manometric pressure at outlet are the specified boundary conditions. Fluid is air and Reynolds number based in the model length  $L$  is  $Re = 2.1 \times 10^6$ .

Three different turbulence models are used with the objective of validate them and verify their differences. The turbulence models are:  $k - \omega$  Standard,  $k - \omega$  SST and Spalart-Allmaras. Default solution parameters from FLUENT are used. Turbulence Specification Method for  $k - \omega$  Standard and  $k - \omega$  SST models is Intensity and Viscosity Ratio with Turbulence Intensity (%) = 0.1 and Turbulence Viscosity Ratio = 1. Turbulence Viscosity Ratio = 1 is used for the Spalart-Allmaras model. The same values of the residuals are used for the three models.

Table 1 shows the computational performance of the turbulence models for the steady flow numerical simulations. It can be seen that the number of iterations and the total CPU time for the  $k - \omega$  Standard are smaller when compared with the other two models. It is interesting to note that despite  $k - \omega$  SST and Spalart-Allmaras models have significantly different numbers of iteration, their total CPU times are almost the same.

Table 2 contains the steady flow simulation results in form of pressure, viscosity and total drag coefficient ( $C_D$ ) for the three proposed turbulence models. Through these results it can be seen that the  $k - \omega$  Standard model is inadequate for the simulated problem, which is a external flow close to the wall. The total  $C_D$  value is around four times the experimental results found in Ahmed (1984) ( $C_{D_{AHMED}} = 0.378$ ) and in present work ( $C_{D_{exp}} = 0.383$ ). The  $k - \omega$  SST and Spalart-Allmaras models result in  $C_D$  values very close to the available experimental results.  $k - \omega$  SST values are closer to the experimental values.

The chosen Ahmed body configuration  $\varphi = 30^\circ$  represents the higher drag case (Fig 2). It has a drag distribution of 85 % due to pressure, and 15 % due to viscosity. Drag distribution for numerical simulations with three different turbulence models is found in Tab. 3. The  $k - \omega$  Standard model overestimates the pressure drag parcel, and this can be one of the causes of the overestimated total drag. The drag distribution for the  $k - \omega$  SST and the Spalart-Allmaras models is closer to that found in Ahmed (1984). These models are adequate to numerical simulation of the steady flow around the Ahmed body.

Table 1. Computational performance for the steady flow numerical simulations

	$k - \omega$ Standard	$k - \omega$ SST	Spalart-Allmaras
Iterations	104	297	451
Total CPU time (s)	6365.25	20459.32	21509.70

Table 2. Steady flow numerical simulation results

	$k - \omega$ Standard	$k - \omega$ SST	Spalart-Allmaras
$C_D$ Pressure	1.533	0.333	0.340
$C_D$ Viscosity	0.085	0.051	0.064
$C_D$ Total	1.618	0.384	0.404

The following figures (Figs. 11 to 14) present the main results of the steady flow numerical simulations. Due to small differences between  $k - \omega$  SST and Spalart-Allmaras results, only the results of the  $k - \omega$  SST model are presented

Table 3. Drag decomposition in parcels due to pressure and viscosity (%)

	Ahmed	$k - \omega$ Standard	$k - \omega$ SST	Spalart-Allmaras
Pressure	85.0	94.7	86.6	84.1
Viscosity	15.0	5.3	13.4	15.9

in these figures. Figure 11 shows some streamlines around the Ahmed body, and the main structure found is a pair of longitudinal vortices. This figure can be compared with the Fig. 8, where it is also evident a longitudinal pair of vortices.

Figures 12 to 14 adopt the same planes presented in Fig. 5. Figure 12 shows the existence of a high pressure region, correspondent to the frontal stagnation point, and a low pressure region along the body and at the rear. The presence of an elevated pressure gradient characterize the Ahmed body as a bluff body in the simulation conditions, and this results that the majority of the drag is due to pressure, as the results of numerical simulations using  $k - \omega$  SST and Spalart-Allmaras turbulence models, and the experimental results found in Ahmed (1984). Figures 13 and 14 present excellent concordance with PIV figures in the EXPERIMENTAL RESULTS section, where it is verified the existence of a recirculation region at the rear of the body and the deflection of the streamlines due to the presence of the body.

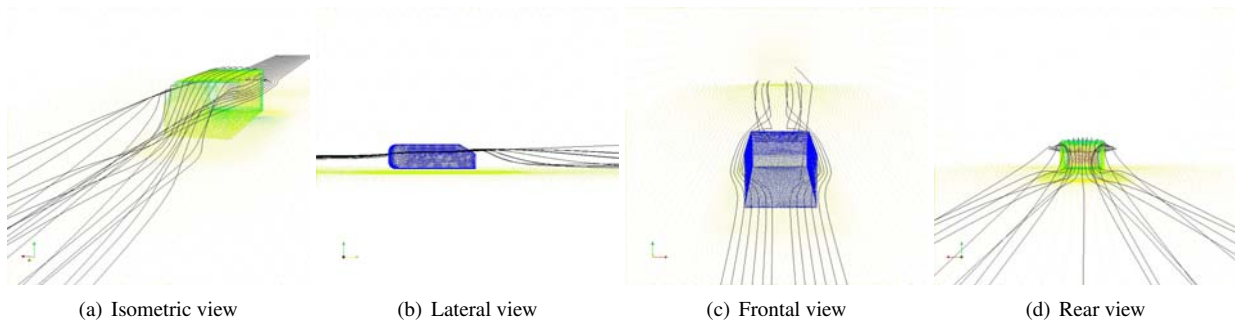


Figure 11. Streamlines around the Ahmed body

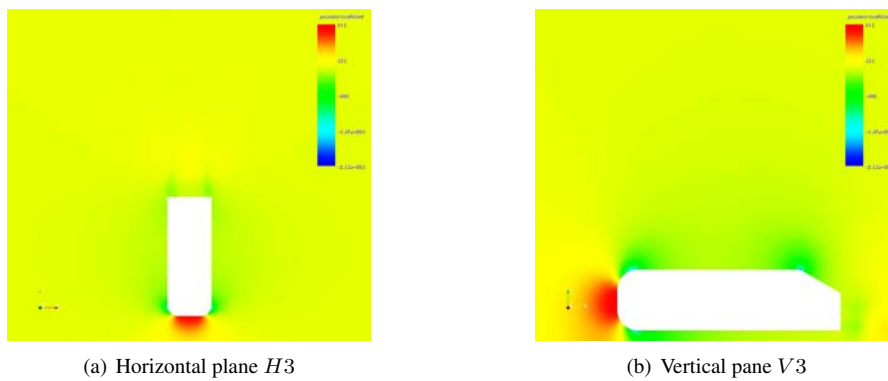


Figure 12. Pressure coefficient distribution around the Ahmed body

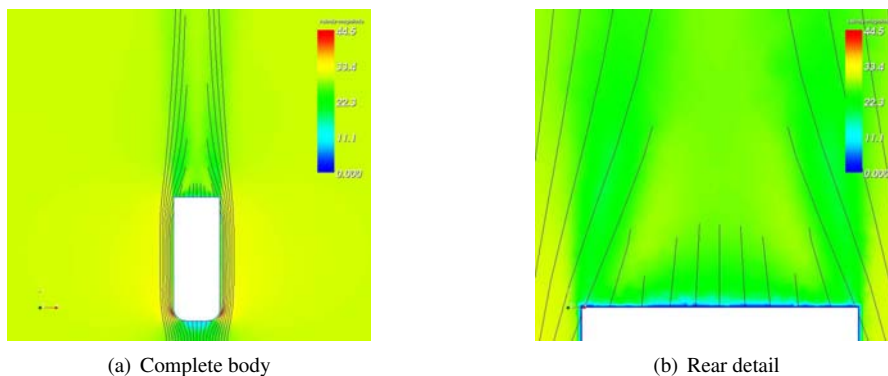


Figure 13. Velocity field and streamlines around the Ahmed body at the plane H3

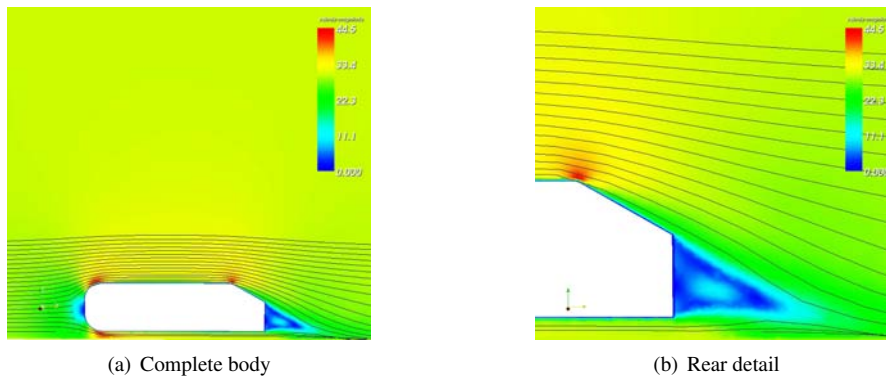


Figure 14. Velocity field and streamlines around the Ahmed body at the plane  $V_3$

### 5.3 Unsteady flow numerical simulations

Computational resources for the unsteady flow numerical simulations are a Compaq Alpha Server DS20E workstation (2 CPUs Alpha EV67 667 MHz and 2GB RAM) and Tru64 Unix V5.1 OS.

Inlet velocity  $V = 30\text{m/s}$  and zero manometric pressure at outlet are the specified boundary conditions. Fluid is air and Reynolds number based in the model length  $L$  is  $Re = 2.1 \times 10^6$ .

Two different turbulence models are used with the objective of validate them and verify their differences. The turbulence models are:  $k - \omega$  SST and Spalart-Allmaras. The  $k - \omega$  Standard turbulence model is not used since its results for the steady flow numerical simulations are not adequate. Default solution parameters from FLUENT are used. Turbulence Specification Method for  $k - \omega$  SST model is Intensity and Viscosity Ratio with Turbulence Intensity (%) = 0.1 and Turbulence Viscosity Ratio = 1. The Turbulence Viscosity Ratio = 1 is used for the Spalart-Allmaras model. The same values of the residuals are used for the two models. Time step size is  $\Delta t = 0.001\text{s}$ , and the number of iterations per time step is 10.

Table 4 shows the computational performance of the turbulence models for the unsteady flow numerical simulations. It can be seen that the Spalart-Allmaras model needs less iterations with a smaller iteration time to reach the same level of convergence obtained by the  $k - \omega$  SST model.

Table 5 contains the unsteady flow simulation results in form of pressure, viscosity and total drag coefficient ( $C_D$ ) for the proposed turbulence models. The  $k - \omega$  SST values are very close to the experimental values, and it is exactly the same value of that found in Ahmed (1984). The Spalart-Allmaras results are overestimated by about 20 %. For the Spalart-Allmaras model, the concordance of the unsteady flow simulations with the experimental results is not quite good as the steady flow simulations. Drag distribution for the numerical simulations with the two different turbulence models is found in Tab. 6, and it is close to that found in Ahmed (1984).

Table 4. Computational performance for the unsteady flow numerical simulations

	$k - \omega$ SST	Spalart-Allmaras
Iterations	410	350
Time steps	41	35
Time per iteration (s)	45	34

Table 5. Unsteady flow numerical simulation results

	$k - \omega$ SST	Spalart-Allmaras
$C_D$ Pressure	0.326	0.397
$C_D$ Viscosity	0.052	0.064
$C_D$ Total	0.378	0.461



Table 6. Drag decomposition in parcels due to pressure and viscosity (%)

	Ahmed	$k - \omega$ SST	Spalart-Allmaras
Pressure	85.0	86.2	86.1
Viscosity	15.0	13.8	13.9

## 6. CONCLUSIONS

This work provide an excellent understanding of the flow characteristics around a bluff body, and more specifically, the Ahmed body, which is important to the automotive industry. The utilization of experimental techniques, as drag measurement and PIV, and computational methods (FVM) permits comparison between two distinct ways of resolution of fluid mechanic problems. Another important results of this paper are comparison of different turbulence models with the available experimental data and verification of their adequacy to a specific problem. The  $k - \omega$  SST and the Spalart-Allmaras models are adequate to simulate the steady flow around the Ahmed body, showing coherent results with the available experimental data. On the other hand, the  $k - \omega$  Standard model is inadequate. Just the  $k - \omega$  SST produces satisfactory results for unsteady flow numerical simulations.

It is evident the importance of the experimental studies to validate the numerical simulations, and that experimental and numerical investigations should coexist whenever it is possible. Actually, this is a tendency that is found in important industries and research departments/institutes.

## 7. ACKNOWLEDGEMENTS

The authors wish to acknowledge the financial support of FAPESP, FINEP, and CNPq, and the technical work related to the model construction carried out by José Guilherme Campetella.

The authors also acknowledge the useful comments and suggestions given by Rafael S. Gioria.

Using resources of the LCCA-Laboratory of Advanced Scientific Computation of the University of São Paulo.

## 8. REFERENCES

- Ahmed, S.R., Ramm, G. and Falin, G., 1984, "Some Salient Features of the Time-Averaged Ground Vehicle Wake", SAE Technical Paper Number 840300.
- ESDU, 2005, "Blockage Corrections for Bluff Bodies in Confined Flows", ESDU, Vol. 1, Number 80024.
- FLUENT INC., 2000, "Gambit Modelling Guide", Version 1.3.
- FLUENT INC., 2005, "Fluent Tutorial Guide".
- Kapadia, S., Roy, S. and Wurtzler, K., 2003, "Detached Eddy Simulation Over a Reference Ahmed Car Model", 41st Aerospace Sciences Meeting and Exhibit, Reno, Nevada, USA.
- Krajnovic, S. and Davidson, L., 2004, "Large Eddy Simulation of the Flow Around an Ahmed Body", ASME Heat Transfer/Fluids Engineering Summer Conference, Charlotte, North Carolina, USA.
- Lienhart, H., Stoots, C. and Becker, S., 2000, "Flow and Turbulence Structures on the Wake of a Similified Car Model (Ahmed Model)", DGLR Fach. Symp. der AG ATAB, Stuttgart University.
- Okada M., Sheridan, J. and Thompson, M., 2005, "Effect of Width-to-Height on Wake Structures of Simplified Vehicle Geometry", Fourth Conference on Bluff Body Wakes and Vortex-Induced Vibrations, Santorini, Greece.

## 9. Responsibility notice

The authors are the only responsible for the printed material included in this paper